Protein regulator of cytokinesis 1 regulates autophagy in hepatitis B virus-associated liver cancer development

JINGJING HUANG[1], XIANZHI CHENG[2], CHUANG WANG[3] and FANGYAN GONG[4]

[1]Department of Infection, Hongqi Hospital Affiliated to Mudanjiang Medical University, Mudanjiang, Heilongjiang157000, P.R. China; [2]Department of Pharmacy, Hongqi Hospital Affiliated to Mudanjiang Medical University, Mudanjiang, Heilongjiang 157000, P.R. China; [3]Department of Neurosurgery, Hongqi Hospital Affiliated to Mudanjiang Medical University, Mudanjiang, Heilongjiang 157000, P.R. China; [4]Department of Clinical Laboratory, Hongqi Hospital Affiliated to Mudanjiang Medical University, Mudanjiang, Heilongjiang 157000, P.R. China

Received April 17, 2024; Accepted January 7, 2025

DOI: 10.3892/or.2025.8869

Abstract. Hepatitis B protein x (HBx) is considered a critical contributor to hepatitis B virus (HBV)-associated liver cancer development. Protein regulator of cytokinesis 1 (PRC1) has been implicated in hepatocarcinogenesis. However, the clinical relevance, biological functions and related regulatory mechanisms of PRC1 in HBV-associated liver cancer have not yet been clarified. PRC1 expression profiles in liver cancer were obtained from The Cancer Genome Atlas and Gene Expression Profiling Interactive Analysis database and through reverse transcription-quantitative polymerase chain reaction and immunohistochemistry assays. A series of *in vitro* and *in vivo* assays were used to explore the function of the PRC1 gene and the possible mechanisms through which it affects HBV-associated liver cancer. PRC1 was overexpressed in HBV-positive liver cancer tissues. Functional studies *in vitro* demonstrated that HBx induced the expression of the PRC1 gene, which promoted cell autophagy and enhanced viability, invasion and migration. Furthermore, the knockdown of the PRC1 gene or treatment with the autophagosome inhibitor 3-methyladenine blocked the HBx-induced autophagic flux, disrupted the formation of autophagosomes, and promoted cell apoptosis. Liver cancer xenograft animal model experiments revealed that inhibition of autophagy by 3-methyladenine or silencing of the PRC1 gene attenuated HBx-induced malignant behavior *in vivo*. The absence of autophagy inhibited the expression of Bcl-2, induced the expression of Bax, and regulated the levels of Th1 and Th2 cytokines. These results elucidate a mechanism wherein the PRC1 gene participates in the occurrence and development of HBV-associated liver cancer by modulating autophagy. PRC1 could be a potential therapeutic target for liver cancer.

Introduction

Liver cancer is recognized as the sixth most prevalent malignancy worldwide, and its incidence rate has been rising in recent decades (1). Statistical studies indicated that 905,677 new cases of liver cancer and 830,180 fatal cases occurred in 2020 worldwide (2). Despite advancements in therapeutic regimens, including antiangiogenic drugs, radiotherapy, chemotherapy, immunotherapy and targeted therapy (3,4), almost 80% of patients with advanced-stage liver cancer are characterized by low response and high recurrence rates, limited overall survival (OS) improvement, and a relative 5-year survival rate of merely 18% (5,6). Hence, exploring the molecular mechanisms underlying liver tumorigenesis is crucial for developing effective treatment strategies.

Liver cancer occurs predominantly in individuals infected with hepatitis B (HBV) and/or C viruses (7). The HBV DNA consists of four regions: C, P, S and X, encoding HBcAg, hepatitis B virus DNA polymerase, HBsAg and hepatitis B virus X protein (HBx), respectively (8,9). HBx, an important small regulatory protein, has attracted researchers' attention. It mainly mediates the transcriptional process by binding to the HBV covalently-closed circular DNA and promotes HBV replication (10). HBx also induces the abnormal expression of proto-oncogenes or oncogenes, regulates autophagy, facilitates cell proliferation, and accelerates the migration and invasion of liver cancer, thereby promoting liver cancer development (11-13). HBx modulates a series of oncogenes that promote the initiation and development of liver cancer and are

Correspondence to: Professor Fangyan Gong, Department of Clinical Laboratory, Hongqi Hospital Affiliated to Mudanjiang Medical University, 5 Tongxiang Road, Aimin, Mudanjiang, Heilongjiang 157000, P.R. China
E-mail: 674768242@qq.com

Abbreviations: HBV, hepatitis B virus; HBx, hepatitis B protein x; OS, overall survival; PRC1, protein regulator of cytokinesis 1; RT-qPCR, reverse transcription quantitative polymerase chain reaction; DAPI, 4'-6-diamidino-2-phenylindole; CCK-8, Cell Counting Kit-8; PI, propidium iodide; 3-MA, 3-methyladenine; IHC, immunohistochemistry; TUNEL, terminal deoxynucleotidyl transferase-mediated nick-end tagging of UTP; ELISA, enzyme-linked immunosorbent assay; TNF-α, tumour necrosis factor-α; IL, interleukin; IFN-γ, interferon-γ

Key words: autophagy, HBx, liver cancer, mechanism, PRC1

closely associated with autophagy (14). Chronic HBV infection is one of the main causative factors for liver cancer; however, the mechanism of HBV-associated liver tumorigenesis is not fully understood and deserves further exploration.

Protein regulator of cytokinesis 1 (PRC1) is localized to the nucleus, cytoplasm and plasma membrane and is an important factor for cytokinesis and cell cleavage (15). Studies have shown that PRC1 is associated with the malignant occurrence and progression of various tumors, including lung adenocarcinoma, ovarian cancer, liver hepatocellular carcinoma (LIHC) and prostate cancer (16-19). However, the role and functional mechanisms of PRC1 in HBV-associated liver cancer remain unknown. An improved understanding could contribute to the development of effective and specific drugs. The present study aimed to explore the effect of the PRC1 gene on autophagy function in human liver cancer cells and elucidate whether it participates in the occurrence and development of HBV-associated liver cancer in an autophagy-dependent manner.

Materials and methods

Patients and samples. Tumor tissues were obtained from 86 patients with liver cancer undergoing primary tumor resection at the Hongqi Hospital Affiliated to Mudanjiang Medical University from June 2018 to April 2022. Among the 86 patients, 43 patients were HBV-positive, and 43 patients were HBV-negative. The present study was approved (approval no. 202052) by the Medical Ethics Committee of Hongqi Hospital Affiliated to Mudanjiang Medical University (Mudanjiang, China), and written informed consent was obtained from each participant. Clinical characteristics (including sex and age distribution) are included in Table I.

Bioinformatics analyses. PRC1 expression profiles in liver cancer were compiled from The Cancer Genome Atlas (http://portal.gdc.cancer.gov) and the Gene Expression Profiling Interactive Analysis (http://gepia.cancer-pku.cn/) databases. Based on the Kaplan-Meier plotter (http://kmplot.com/analysis), the OS rate of patients with liver cancer was determined.

Cell culture. The human liver cancer cell lines, Huh7 (HBV-negative) and HepG2 (HBV-negative), were purchased from Chinese Academy of Sciences Cell Bank of Type Culture Collection. Cells were cultured in Dulbecco's modified Eagle's medium (DMEM; Thermo Fisher Scientific, Inc.) containing 10% fetal bovine serum (FBS; Thermo Fisher Scientific, Inc.) and 1% penicillin-streptomycin (100 IU/ml; Thermo Fisher Scientific, Inc.) at 37˚C in a humidified incubator under 5% CO_2. The Huh7 and HepG2 cells underwent annual short tandem repeat (STR) profiling analysis, population doubling time and morphology for genetic confirmation. All experiments were performed with early-passage cells (passages 3-10).

Transfection of small interfering RNA (siRNA). The siRNA oligonucleotides were obtained from General Biology Co., Ltd. (www.generalbiol.com). The primer sequences of the siRNAs were as follows: PRC1-Homo-1816 sense, 5'-GGAAAGCGC UGCAAUUAGATT-3' and antisense, 5'-UCUAAUUGCAGC GCUUUCCTT-3'; negative siRNA sense, 5'-GUACCGCAC GUCAUUCGUAUC-3' and antisense, 5'-UACGAAUGACGU GCGGUACGU-3'. According to the manufacturer's protocol, 50 nM of siRNAs were mixed with 125 μl of Opti-MEM™. Additionally, 5 μl of lipofectamine 2000 (Invitrogen; Thermo Fisher Scientific, Inc.) was added to 125 μl of Opti-MEM™ and incubated for 5 min at 25˚C. The solution containing siRNA was then mixed with solution containing lipofectamine 2000 and incubated for 15 min at ambient temperature. The siRNA/liposome 2000 complex was added to six-well plates at 250 μl per well and incubated for 48 h at 37˚C. Cells were collected for further analysis and the silencing efficiency of the PRC1 siRNA vector have been confirmed (Fig. S1).

Plasmids and recombinant adenoviruses. PRC1 cDNA or HBx DNA fragments were subcloned into a pcDNA3.1 mammalian expression vector (Invitrogen; Thermo Fisher Scientific, Inc.). The primer sequences of the pcDNA3.1-PRC1 (pc-PRC1) plasmid were as follows: PRC1 sense, 5'-ACACTCTGTGCA GCGAGTTAC-3' and antisense, 5'-TTCGCATCAATTCCA CTTGGG-3'. The primers for the pcDNA3.1-HBx (pc-HBx) plasmid were as follows: HBx sense, 5'-GGGACGTCCTTT GTCTACGT-3' and antisense, 5'-GGGAGACCGCGTAAA GAGAG-3'. The reconstituted pc-HBx, pc-PRC1, and empty [pc-negative control (NC)] plasmids were transfected into Huh7 and HepG2 cells. Briefly, pc-HBx, pc-PRC1, or pc-NC plasmids mixed with lipofectamine 2000 were incubated with cells for 6 h and then cultured in DMEM containing 20% FBS for 48 h. Plasmids (2.5 μg/ml) were used for cellular viability, migration, invasion and apoptosis assays. The overexpression efficiency of the pc-PRC1 and pc-HBx plasmid was confirmed (Figs. S2 and S3).

Reverse transcription-quantitative polymerase chain reaction (RT-qPCR). RNAiso Plus (Takara Biotechnology Co., Ltd.) was applied to extract total RNA from liver cancer tissues. Subsequently, reverse transcription was performed using the HiScript III qRT SuperMix kit (Vazyme Biotech Co. Ltd.) according to the manufacturer's protocol. The relative level of PRC1 was normalized to β-actin using the threshold cycle ($2^{-\Delta\Delta CT}$) method (20). The specific primer sequences were as follows: PRC1 sense, 5'-GCTGAGATTGTGCGGTTA-3' and antisense, 5'-GCCTTCAACTCTTCTTCCA-3'; β-actin sense, 5'-ACGTGGACATCCGCAAAGAC-3' and antisense, 5'-CTG CTGTCACCTTCACCGTTC-3'. The following optimal thermal cycling conditions were used: 95˚C for 3 min, followed by 30 cycles of 95˚C for 1 min, 60˚C for 1 min and 72˚C for 1 min.

Western blot analysis. Huh7 and HepG2 cells were harvested and lysed in RIPA buffer supplemented with 1 mM phenyl-methyl-sulfonyl fluoride (Beyotime Institute of Biotechnology). Protein concentrations were assessed using the bicinchoninic acid (BCA) method. An equal amount of protein (20 μg) was separated using 12% sodium dodecyl sulfate-polyacrylamide gel electrophoresis, transferred to a polyvinyl difluoride membrane (MilliporeSigma). After blocking with 5% skimmed milk for 2 h at room temperature, the membranes were immunoblotted with primary antibodies specific to PRC1 (1:3,000; cat. no. PA1-27244; Thermo Fisher Scientific, Inc.)

Table I. Relationship between PRC1 protein expression and clinicopathological characteristics of liver cancer.

Characteristics	Expression level of PRC1		Chi-square	P-value
	Low (n=44) (%)	High (n=42) (%)		
Age, years			0.330	0.566
≤55	14 (31.8)	11 (26.2)		
>55	30 (68.2)	31 (73.8)		
Sex			0.361	0.548
Male	31 (70.5)	32 (76.2)		
Female	13 (29.5)	10 (23.8)		
Tumor volume, cm^3			0.171	0.679
≤5	19 (43.2)	20 (47.6)		
>5	25 (56.8)	22 (52.4)		
Pathological stage			4.872	0.027
I~II	34 (77.3)	23 (54.8)		
III~IV	10 (22.7)	19 (45.2)		
Differentiation grade			4.769	0.029
High	33 (75)	22 (52.4)		
Low	11 (25)	20 (47.6)		
Cirrhosis			0.385	0.535
Yes	27 (61.4)	23 (54.8)		
No	17 (38.6)	19 (45.2)		
Lymph node metastasis			3.965	0.046
Yes	10 (22.7)	18 (42.9)		
No	34 (77.3)	24 (57.1)		
Alpha-fetoprotein, μg/l			5.18	0.023
≤400	36 (81.8)	25 (59.5)		
>400	8 (18.2)	17 (40.5)		

PRC1, protein regulator of cytokinesis 1.

and ATG5 (1:500; cat. no. NB110-53818; Novus Biologicals, LLC) overnight at 4˚C. Afterward, the membranes were incubated with horseradish peroxidase-conjugated secondary antibodies (1:1,000; cat. no. A0216; Beyotime Institute of Biotechnology) for 1 h at room temperature. Subsequently, an enhanced chemiluminescence western detection system (Cell Signaling Technology, Inc.) was used to detect band intensities, and the bands densities were analyzed with ImageJ software 1.8.0 (National Institutes of Health).

Immunofluorescence analysis. Huh7 and HepG2 cells ($5.0x10^6$ cells/ml) climbing slices were placed in a 6-well plate and fixed with 4% paraformaldehyde for 30 min at room temperature, permeabilized, and blocked with 0.1% Triton X-100 in 5% bovine serum albumin (Beijing Solarbio Science & Technology Co., Ltd.) solution for 30 min. The samples were treated with primary antibody against PRC1 (1:500; cat. no. 15617-1-AP; ProteinTech Group, Inc.) or LC3B (1:500; cat. no. 14600-1-AP; ProteinTech Group, Inc.) overnight at 4˚C, followed by incubation with FITC-conjugated secondary antibody (1:200; cat. no. SA00003-2; ProteinTech Group, Inc.) for 1 h at ambient temperature. Nuclei were counterstained with 100 μl 4'-6-diamidino-2-phenylindole (DAPI; 1 μg/ml; Beyotime Institute of Biotechnology). Cells were visualized with a confocal laser scanning microscope (Olympus Corporation).

Autophagy flux assay. An mCherry-GFP-LC3 reporter was used to observe autophagosome formation and autophagic flux. Autophagosome formation leads to an increase in yellow spots, while autolysosome formation leads to an increase in red spots. Briefly, cells were infected with adenovirus encoding mCherry-GFP-LC3 for 2 h and then visualized with a confocal laser scanning microscope. The number of LC3-positive puncta per cell in GFP-positive or mCherry-GFP-positive cells was determined.

Electron microscopy. Huh7 and HepG2 cells were harvested, centrifuged in 1 mm^3 blocks, and soaked in 2.5% glutaraldehyde solution for 2 h. The pellets were post-fixed in 1% osmium tetroxide (Ted Pella; www.tedpella.com) for 1 h, dehydrated in graded alcohol solutions (50, 70, 90, 96 and 100%), and embedded in Eponate 12 resin (Ted Pella). Ultrathin (70~80 nm) sections were prepared and stained with 5%

uranyl acetate (Ted Pella) and lead citrate (Ted Pella) for 1 h at ambient temperature. The ultrastructure of Huh7 and HepG2 cells was visualized using a transmission electron microscope (JEM 1011; JEOL, Ltd.).

Cell viability assay. The Cell Counting Kit-8 (CCK-8; Dojindo Laboratories, Inc.) assay was used to assess cell viability. Briefly, Huh7 and HepG2 cells were transfected with 2.5 μg/ml pc-PRC1 or pc-NC. After 48 h, the cells were plated into a 96-well plate at 5,000 cells per well. After 48-h incubation, 100 μl of culture medium supplemented with 10 μl CCK-8 solution was added into each well and then incubated for 2 h at 37˚C. The optical density at 450 nm was detected using a BioTek Synergy H^1 Microplate Reader (BioTek Instrument Inc.).

Cell apoptosis assay. Huh7 and HepG2 cells were transfected with 50 nM PRC1 siRNA or negative control siRNA or exposed to 5 mM 3-MA for 48 h, and then transfected with 2.5 μg/ml pc-HBx for another 48 h. Cells ($5x10^5$ cells/ml) were harvested and incubated with 5 μl of Annexin V and 5 μl of propidium iodide (PI) (Vazyme Biotech Co., Ltd.) for 25 min in the dark. Then, apoptotic cells were detected using a FacsCalibur flow cytometer (BD Biosciences), and the results were analyzed using the software CellQuest version 3.3 (BD Biosciences).

Cell invasion assay. The invasion of cells was detected using Transwell chambers (6-well plate, 8-μm pore size). The cell invasion chambers were precoated by placing 100 μl Matrigel (1:5 dilution) onto the filter, and incubating the filter for 30 min at 37˚C to allow Matrigel polymerization. Huh7 and HepG2 cells were transfected with 2.5 μg/ml pc-PRC1 or pc-NC. After 48 h, starved cells ($5x10^5$ cells/ml) were seeded into the top chamber, while 500 μl of DMEM containing 20% FBS was filled into the lower chamber. After 48 h, the invasive cells were stained with 0.1% crystal violet for 20 min at ambient temperature. The invasive ability of Huh7 and HepG2 cells was then determined under a light microscope (magnification, x200; Olympus Corporation).

Cell migration assay. The wound-healing assays was used to assess the migratory ability of Huh7 and HepG2 cells. Cells were transfected with 2.5 μg/ml pc-PRC1 or pc-NC for 48 h and then reseeded into 6-well plates. Once cells reached ~80-90% confluence, the monolayer of cells was scratched in a straight line on the surface (at time point 0). Subsequently, the cells were cultured in serum-free medium in a 5% CO_2 incubator at 37˚C (21). The healing width of the wound was observed at 48 h under a light microscope (magnification, x200; Olympus Corporation).

In vivo subcutaneous xenograft assay. HepG2 cells were transfected with PRC1 siRNA (50 nM) or negative control siRNA (50 nM) or exposed to the autophagosome inhibitor 3-methyladenine (3-MA, 5 mM) for 48 h, and then transfected with pc-HBx (2.5 μg/ml) for another 48 h. A total of 20 5-week-old male BALB/c-nu mice weighing 18-23 g (four mice per group, Liaoning Changsheng biotechnology Co., Ltd.) were used. All animals were housed in a specific pathogen-free animal facility and maintained in a temperature and humidity-controlled environment (~20-22˚C, 40~60% humidity) with free access to food and water in a lighting cycle of 12 h darkness/12 h light. A total of 100 μl sterile PBS containing $1x10^7$ HepG2 cells were processed and then subcutaneously injected into the right flank of the mice. Xenograft tumor growth was recorded every 2 days; when the tumor volume reached 100~150 mm^3, the mice were humanely sacrificed by intraperitoneal injection of pentobarbital (100 mg/kg). Tumor tissues were collected and weighed. Paraformaldehyde-fixed and paraffin-embedded tumor tissues were cut into sections for immunohistochemistry (IHC). The animal care committee at Mudanjiang Medical University (Mudanjiang, China) approved the present study (approval no. 2022-500-177). All animals received human care, and the study protocols complied with the institution's guidelines.

IHC. The liver cancer tissues were fixed in 4% paraformaldehyde and embedded in paraffin, and then processed and sectioned. IHC was conducted by Wuhan Servicebio Technology Co., Ltd. Primary monoclonal antibodies against PRC1 (1:500) were added to the paraffinized slides, probed with HRP-labeled antibodies (1:50; cat. no. A0216; Beyotime Institute of Biotechnology), and visualized with 3, 3'-diaminobenzidine. Subsequently, the cell nuclei were stained with blue hematoxylin for 5 min at ambient temperature for histochemical assessment. The expression level of PRC1 was calculated based on the staining intensity score (strong staining: 3; moderate staining: 2; weak staining: 1) multiplied by a score of the percentage of positive cells (4, >75%; 3, 51~75%; 2, 25~50%; 1, <25%), resulting in an IHC score of between 1 and 12. As outlined in Table I, an IHC score ≥6 indicated a high expression of PRC1, whereas a score <6 was considered a low expression of PRC1.

Paraffin-embedded slides of subcutaneous tumors from xenograft mice were treated with ATG5 (1:400; cat. no. NB110-53818; Novus Biologicals, LLC), Bax (1:500; cat. no. 3351; ProSci; www.prosci-inc.com), and Bcl-2 (1:1,000; cat. no. NB100-56098; Novus Biologicals, LLC) antibodies overnight at 4˚C. A light microscope (Carl Zeiss AG) was used to observe and acquire images of the stained tissues. The H-score in the measurement area was calculated as follows: H-Score=(percentage of strong-intensity area x3) + (percentage of moderate-intensity area x2) + (percentage of weak-intensity area x1).

Terminal deoxynucleotidyl transferase dUTP nick end labeling (TUNEL) analysis. The apoptotic rate in the xenograft tumor tissues was evaluated using a TUNEL assay kit (cat. no. 11684795910; Roche Diagnostics GmbH) following the manufacturer's protocols. Paraffin-embedded slides of subcutaneous tumors were treated with 4% H_2O_2 for 25 min and then incubated with 50 μl of TUNEL reaction solution and 50 μl of peroxidase-conjugated antibodies for another 25 min. The slides were reacted with 50 μl of 0.05% diaminobenzidine solution, and the apoptotic rate was observed using inverted fluorescence microscope (Olympus Corporation).

Enzyme-linked immunosorbent assay (ELISA). The levels of Th1 cytokines tumor necrosis factor-α (TNF-α; cat. no. MTA00B), interleukin (IL)-2 (cat. no. QK202),

interferon-γ (IFN-γ; cat. no. QK285) and Th2 cytokines IL-6 (cat. no. D6050B), IL-10 (cat. no. M1000B) and IL-4 (cat. no. M4000B) in mice serum were detected using ELISA kits (R&D Systems, Inc.) according to the manufacturer's protocols.

Statistical analysis. Statistical analysis was performed using SPSS software version 13.0 (SPSS Inc.). Quantitative results are presented as the mean ± standard deviation. Unpaired Student's t-test was used to analyze the differences between two groups, and one-way analysis of variance was used to compare more than two groups, and Tukey's post-hoc test was employed for further statistical assessment. In Table I, the Chi-square test was performed to analyze clinical data. $P<0.05$ was considered to indicate a statistically significant difference.

Results

Characteristics of the PRC1 gene in liver cancer tissues. The expression of the *PRC1* gene was evaluated in human pan-cancer using dot plot analysis (Fig. 1A). The results indicated that compared with adjacent normal tissues, the PRC1 gene was highly expressed in most tumor tissues, including bladder urothelial carcinoma, breast invasive carcinoma, head and neck squamous cell carcinoma, cervical squamous cell carcinoma, LIHC and lung squamous cell carcinoma. Box plots revealed that PRC1 gene expression in liver cancer tissues (369 cases) was significantly higher than that in normal liver tissue (160 cases, Fig. 1B). Pathological stage plot indicated an association between PRC1 mRNA expression and the tumor pathological stage (Pr (>F)=0.000142; Fig. 1C). The association between PRC1 gene expression and OS in patients with liver cancer (364 cases) was analyzed using the Kaplan-Meier plotter. High PRC1 gene expression was associated with shorter OS in patients with liver cancer (Log rank P=0.00038; Fig. 1D). Moreover, Kaplan-Meier plots demonstrated a PRC1 gene hazard ratio (HR) of 1.9 (where factors with an HR >1 are considered a risk factor for the disease), supporting its importance as a hazard factor for liver cancer. IHC and RT-qPCR indicated that PRC1 expression in HBV-positive tumor tissues was higher than in HBV-negative tumor tissues (Fig. 1E and F). An association between PRC1 expression level and baseline demographics of patients with liver cancer is presented in Table I. The chi-square test indicated that high PRC1 expression levels were significantly associated with pathological stage III-IV, low differentiation, lymph node metastasis and alpha-fetoprotein (AFP) >400 μg/l.

PRC1 gene enhances cell autophagy and induces malignant phenotypes in vitro. To identify the role of the *PRC1* gene in liver cancer development, the effect of its upregulation on autophagy was assessed in Huh7 and HepG2 cells. The autophagy-associated ATG5 protein level was determined using western blot analysis (Fig. 2A). The present findings demonstrated that the pc-PRC1 treatment significantly increased the level of ATG5 relative to the mock treatment ($P<0.01$). Further examination using a plasmid encoding mCherry-GFP-LC3B identified higher autophagic flux (the rate of red puncta formation in each cell) in the cytoplasm of Huh7 and HepG2 cells treated with pc-PRC1 but low (basal) autophagic flux in mock-treated cells or cells treated with pc-NC (Fig. 2B). The viability of Huh7 and HepG2 cells transfected with pc-PRC1 was significantly higher than in the mock treatment ($P<0.01$; Fig. 2C). Moreover, the Transwell and scratch tests showed that compared with mock treatment, the pc-PRC1 treatment significantly increased the number of invasive cells and enhanced the migration distance ($P<0.01$; Fig. 2D and E).

Effect of the PRC1 gene on autophagy and apoptosis in HBx-treated Huh7 and HepG2 cells. To evaluate whether the PRC1 gene plays an important role in HBV-positive liver cancer, the effect of pc-HBx treatment was first assessed on PRC1 protein expression in Huh7 and HepG2 cells. As shown in Fig. 3A, PRC1 protein expression in the pc-HBx treatment group was significantly higher than in the pc-NC group ($P<0.01$). Furthermore, the FITC-labelled PRC1 protein was primarily located in the cytoplasm of Huh7 and HepG2 cells in the HBx and HBx + negative siRNA treatments, while it rarely appeared in cells treated with HBx + PRC1 siRNA or HBx + 3-MA (Fig. 3B). To further assess the role of the PRC1 gene in HBx-treated Huh7 and HepG2 cells, the autophagic flux was detected using the mCherry-GFP-LC3B plasmid. The data revealed that the HBx and HBx + negative siRNA treatments potently enhanced the autophagic flux, while autophagic flux was rarely observed in the HBx + PRC1 siRNA and HBx + 3-MA treatments (Fig. 3C). Consistent with these results, electron microscopy demonstrated autophagosomes in the HBx and HBx + negative siRNA treatments. By contrast, the HBx + PRC1 siRNA and HBx + 3-MA treatments eliminated these adverse effects and restored normal mitochondrial morphology (Fig. 3D). Finally, cell apoptotic level was measured by annexin V-fluorescein isothiocyanate/PI staining. As shown in Fig. 3E, the cell apoptotic rate in the HBx + PRC1 siRNA group was significantly higher than in the HBx and HBx + negative siRNA groups ($P<0.01$). However, the HBx + PRC1 siRNA and HBx + 3-MA groups had similar cell apoptotic rates.

Effect of the PRC1 gene on autophagy and apoptosis in an HBx-treated murine xenograft model. HepG2 cells overexpressing the HBx gene or with silenced PRC1 gene expression were subcutaneously injected into nude mice to assess the role of PRC1 in liver cancer *in vivo*. TUNEL assays indicated that the apoptotic rate in the HBx + PRC1 siRNA group was significantly higher than in the HBx and HBx + negative siRNA groups ($P<0.01$). However, similar apoptotic rates were observed in the HBx + PRC1 siRNA or HBx + 3-MA groups ($P>0.05$; Fig. 4A). IHC assays demonstrated that the expression of ATG5 and Bcl-2 after the HBx + PRC1 siRNA treatment was significantly lower than compared with HBx and HBx + negative siRNA treatments ($P<0.01$). However, the HBx + PRC1 siRNA and HBx + 3-MA treatment groups had similar ATG5 and Bcl-2 expression levels ($P>0.05$). Bax protein levels in the HBx + PRC1 siRNA treatment group were significantly higher than those in the HBx and HBx + negative siRNA treatment groups ($P<0.01$). However, the HBx + PRC1 siRNA and HBx + 3-MA groups had similar Bax expression levels ($P>0.05$; Fig. 4B).

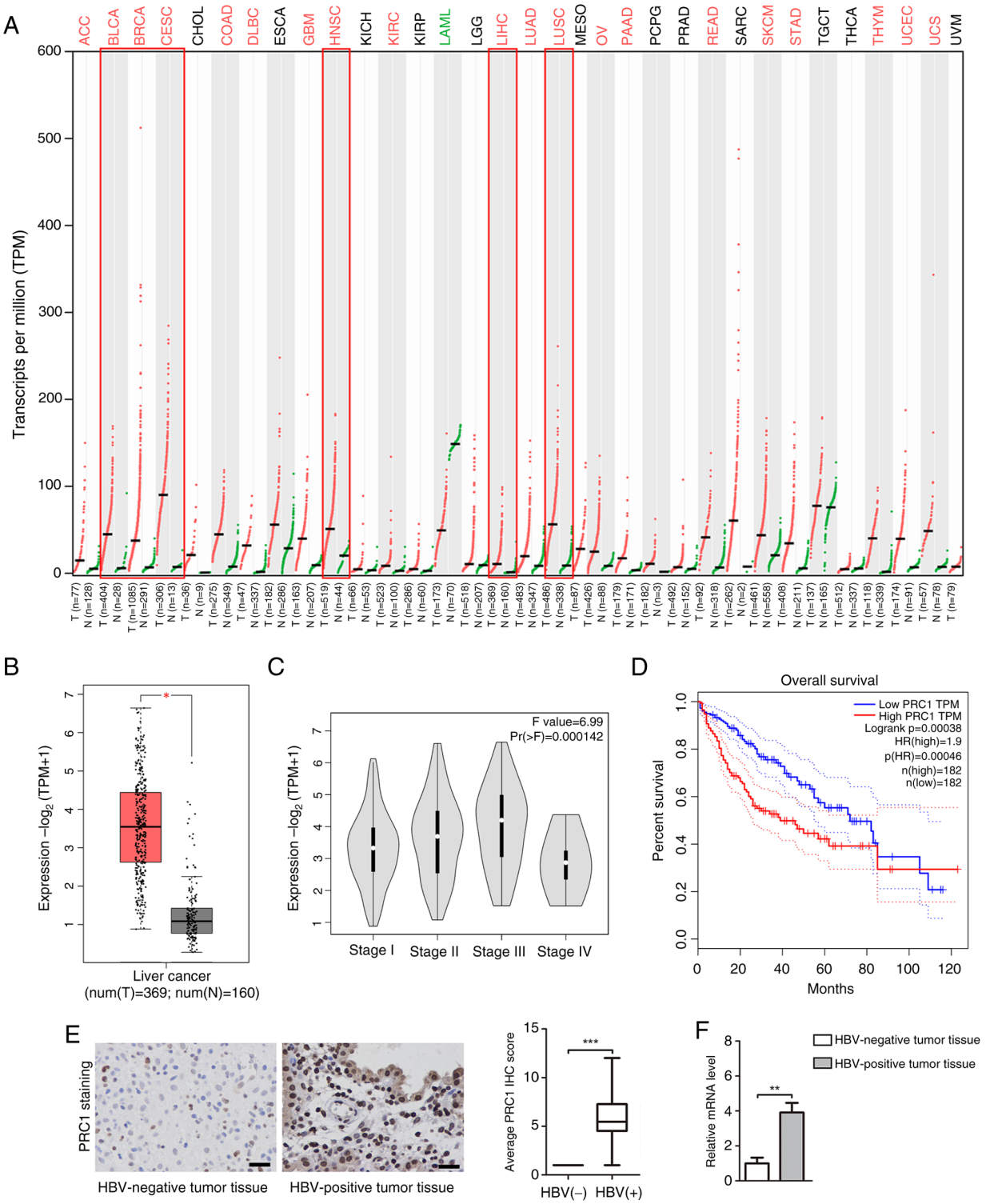

Figure 1. Characteristics of the PRC1 gene in liver cancer tissues. (A) The expression of the PRC1 gene was evaluated in human pan-cancer using dot plot analysis. (B) PRC1 gene expression in box plot, including 369 cases of liver cancer tissues and 160 cases of normal tissues. Data were acquired from the Genotype-Tissue Expression project and are shown as the mean ± quartile values. *P<0.05 by the unpaired Student's t-test. (C) Relationship between PRC1 gene expression and tumor pathological stage was presented in pathological stage plot. (D) The association between PRC1 gene expression and overall survival in patients with liver cancer (364 cases) was analyzed using the Kaplan-Meier plotter. (E) The expression of PRC1 protein in HBV-positive tumor tissues and HBV-negative tumor tissues was measured using immunohistochemical staining (magnification, x400). Brown indicates positive staining (Scale bars, 50 μm). (F) The mRNA level of PRC1 was detected using the reverse transcription-quantitative PCR assay. **P<0.01 and ***P<0.001 vs. the HBV-negative tumor tissues. PRC1, protein regulator of cytokinesis 1; HBV, hepatitis B virus; ACC, adenoid cystic carcinoma; BLCA, bladder urothelial carcinoma; BRCA, breast invasive carcinoma; CESC, cervical squamous cell carcinoma and endocervical adenocarcinoma; CHOL, cholangiocarcinoma; COAD, colon adenocarcinoma; DLBC, diffuse large B-cell lymphoma; ESCA, esophageal carcinoma; GBM, glioblastoma multiforme; HNSC, head and neck squamous cell carcinoma; KICH, kidney chromophobe; KIRC, kidney renal clear cell carcinoma; KIRP, kidney renal papillary cell carcinoma; LGG, low-grade glioma; LIHC, liver hepatocellular carcinoma; LUAD, lung adenocarcinoma; LUSC, Lung squamous cell carcinoma; MESO, mesothelioma; OV, ovarian serous cystadenocarcinoma; PAAD, pancreatic adenocarcinoma; PCPG, pheochromocytoma and paraganglioma; PRAD, prostate adenocarcinoma; READ, rectum adenocarcinoma; SARC, sarcoma; SKCM, skin cutaneous melanoma; STAD, stomach adenocarcinoma; TGCT, testicular germ cell tumors; THCA, thyroid carcinoma; THYM, thymoma; UCEC, uterine corpus endometrial carcinoma; UCS, uterine carcinosarcoma; UVM, uveal melanoma.

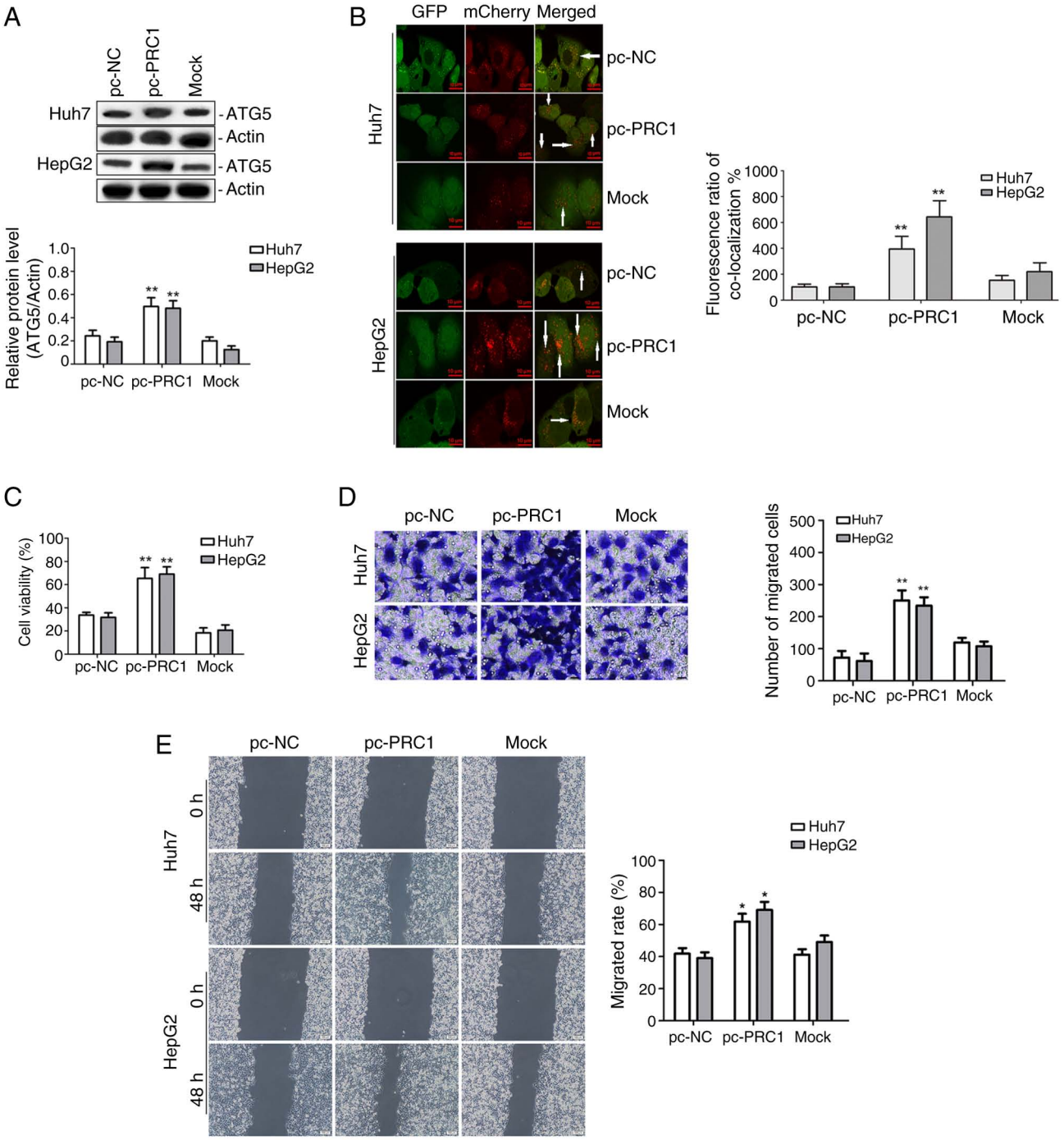

Figure 2. Effect of the PRC1 gene on malignant phenotypes in Huh7 and HepG2 cells. Huh7 and HepG2 cells were transfected with 2.5 μg/ml pc-PRC1 or pc-NC for 48 h. (A) The autophagy-associated ATG5 protein level was detected using western blot analysis. Relative protein expression was normalized to that of actin (n=3). (B) Autophagic flux (white arrow) in Huh7 and HepG2 cells was monitored by laser confocal microscopy using the mCherry-GFP-LC3 reporter. Scale bars, 10 μm. (C) The viability of Huh7 and HepG2 cells was measured using the Cell Counting Kit-8 assay. (D) The invasion of Huh7 and HepG2 cells was detected by the Transwell assay. (E) The migration of Huh7 and HepG2 cells was analyzed by the wound healing assay (n=3). *P<0.05 and **P<0.01 vs. mock treatment. PRC1, protein regulator of cytokinesis 1; NC, negative control.

Cytokines are an important factor in inflammatory responses during liver tumorigenesis. Treatment with HBx + PRC1 siRNA significantly induced the levels of IL-10, IL-4 and IL-2 and suppressed the levels of IL-6, TNF-α and IFN-γ relative to treatment with HBx or HBx + negative siRNA (all P<0.05). However, the HBx + PRC1 siRNA and HBx + 3-MA treatment groups had similar levels of the Th1 and Th2 cytokines (P>0.05; Fig. 4C). These results suggest that the PRC1 gene regulates the release of cytokines in HBx-associated liver cancer.

Discussion

There is a significant association between the sustained replication of HBV and the malignant phenotypes of liver cancer in humans (14). The present study explored the role

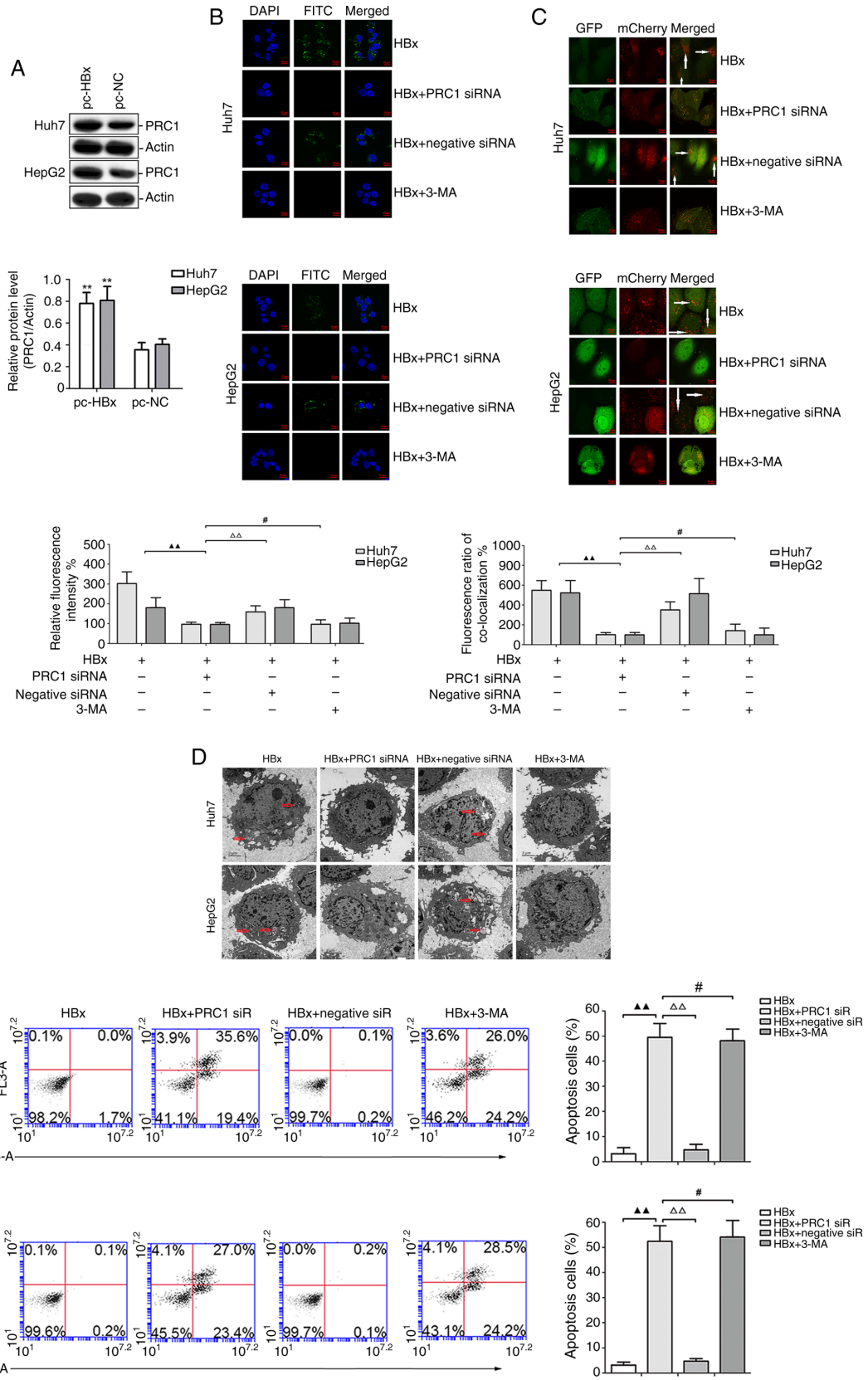

Figure 3. Effect of the PRC1 gene on autophagy and apoptosis in HBx-treated Huh7 and HepG2 cells. Huh7 and HepG2 cells were transfected with 2.5 μg/ml pc-HBx or pc-NC for 48 h. (A) The PRC1 protein level was measured using western blot analysis. Relative protein expression was normalized to that of actin (n=3). **P<0.01 vs. the pc-NC group. Huh7 and HepG2 cells were transfected with 50 nM PRC1 siRNA or negative control siRNA or exposed to 5 mM 3-MA for 48 h, and then transfected with 2.5 μg/ml pc-HBx for another 48 h. (B) FITC-labelled PRC1 protein (green) was observed using laser confocal microscopy. Nucleus was stained with DAPI (blue). Scale bars, 10 μm. (C) Images of autophagic flux in Huh7 and HepG2 cells were captured by laser confocal microscopy using the mCherry-GFP-LC3 reporter. Scale bars, 10 μm. (D) The morphology of autophagosomes was observed using electron microscopy (x2500). Red arrows indicate autophagosome formation. Scale bar, 2 μm. (E) The apoptosis of Huh7 and HepG2 cells was measured by flow cytometry (n=3). $^{▲▲}$P<0.01 vs. HBx treatment; $^{\#}$P>0.05 and $^{△△}$P<0.05 vs. HBx and PRC1 siRNA co-treatment. PRC1, protein regulator of cytokinesis 1; HBx, hepatitis B protein x; NC, negative control; siRNA, small interfering RNA; 3-MA, 3-methyladenine.

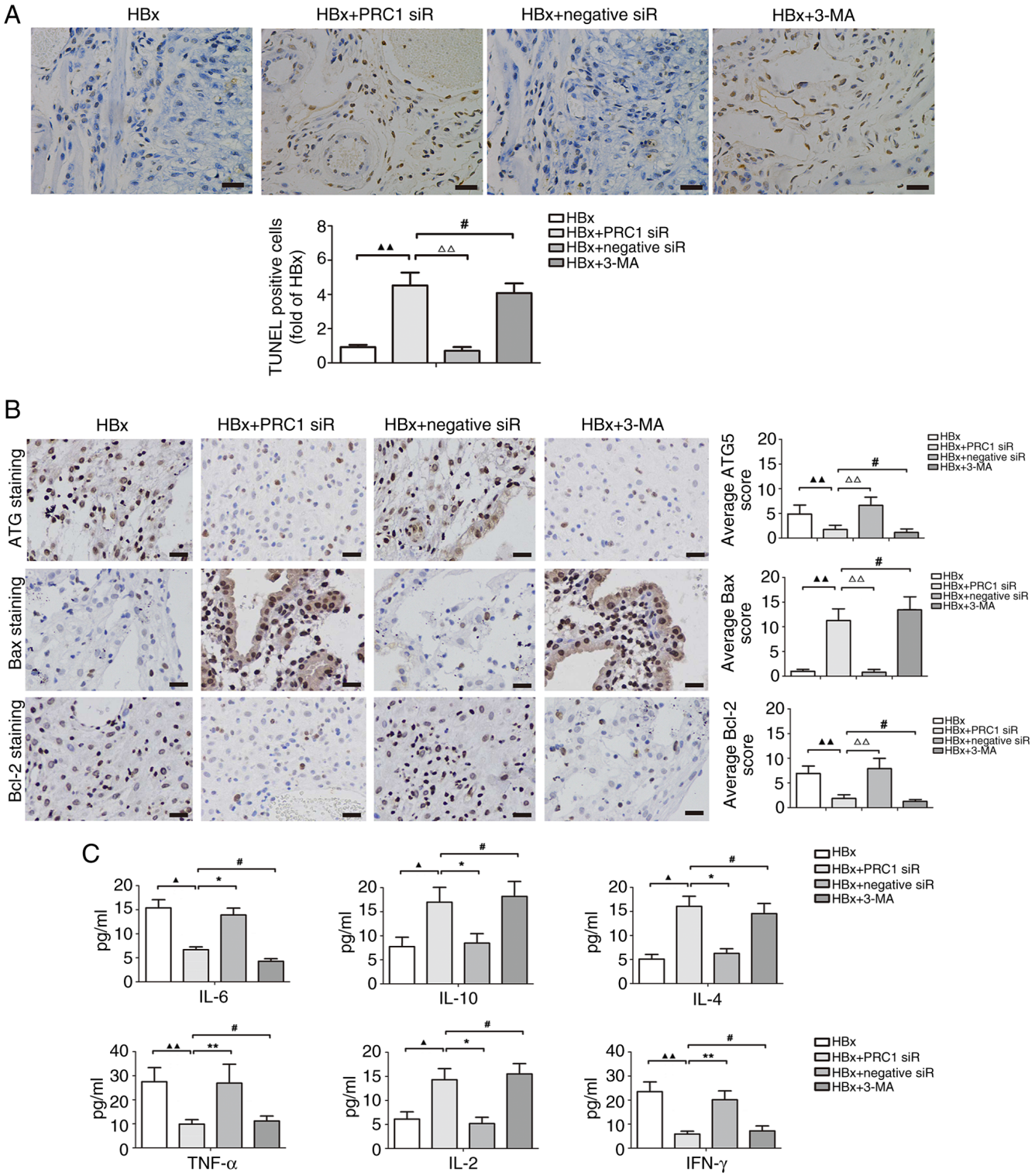

Figure 4. Effect of the PRC1 gene on autophagy and apoptosis in an HBx-treated murine xenograft model. (A) Apoptosis of tumor tissues was measured by TUNEL assay. The apoptotic cells are stained brown. Scale bars, 50 μm. (B) The expression of autophagy-related protein ATG5 and apoptosis-related proteins Bax, Bcl-2 in tumor tissues was observed using immunohistochemical staining. Brown indicates positive staining. Scale bars, 50 μm. $^{▲▲}$P<0.01 vs. HBx treatment; $^{\#}$P>0.05 and $^{△△}$P<0.01 vs. HBx and PRC1 siRNA co-treatment. (C) The levels of Th1 cytokines (TNF-α, IL-2 and IFN-γ) and Th2 cytokines (IL-6, IL-10 and IL-4) in the mice serum were detected by ELISA. $^{▲}$P<0.05 and $^{▲▲}$P<0.01 vs. HBx treatment; $^{\#}$P>0.05, *P<0.05 and **P<0.01 vs. HBx and PRC1 siRNA co-treatment. PRC1, protein regulator of cytokinesis 1; HBx, hepatitis B protein x; siRNA, small interfering RNA; TNF-α, tumour necrosis factor-α; IL, interleukin; IFN-γ, interferon-γ; 3-MA, 3-methyladenine.

of the PRC1 gene in the occurrence and development of HBV-associated liver cancer. Exploring target molecules that simultaneously regulate HBV and liver cancer could be a feasible strategy to overcome these two closely related diseases (22). In summary, the findings of the present study indicate that PRC1 gene expression sensitively responds to HBV infection and hence serves as an ideal prospective target for liver cancer treatment.

HBV is a major risk factor for liver tumorigenesis and is closely related to the survival and prognosis of patients with liver cancer. HBV-associated liver cancer accounts for ~50~60% of liver cancer cases (23,24). Numerous HBV genotypes have exhibited varying degrees of autophagic activity augmentation (25). It has been reported that HBV activates autophagy mainly in an HBx protein-dependent manner (26). HBx is a multifunctional regulatory protein involved in regulating viral replication and cellular functions, such as cell proliferation, apoptosis, differentiation, transformation, autophagy and DNA repair (10,27). Autophagy is a crucial homeostatic pathway that promotes the degradation and recycling of cellular substances (28). However, autophagy has dual functions in cancer, in the tumor cells (intrinsic) and in the surrounding matrix (extrinsic), depending on the tumor staging, specific oncogenic mutations and the surrounding microenvironment (29). It was previously indicated that autophagy plays a suppressive role in liver cancer development. The deletion of the ATG5 or liver-specific ATG7 gene in mice resulted in the development of liver tumors (30). Furthermore, expression of the autophagy-related Beclin 1 protein in liver tumors was lower than in adjacent normal tissues (31). However, Qian *et al* (32) pointed out that autophagy shifted from a suppressive role to a promoter role in the late stage of liver cancer by suppressing the expression of p53 and p21. The current study demonstrated the mechanism by which autophagy affects HBV-related tumorigenesis and its significance for potential treatments.

Autophagy maintains cell metabolism and enhances the resistance to hypoxia and nutrient deprivation. By alleviating cellular stress, autophagy allows cancer cells to survive through therapy or, occasionally, enter a dormant state (33). Activation of the epithelial-mesenchymal transition-related transcription factors Slug and Snail causes the acquisition of a cancer-initiating cells phenotype and activates autophagy (34). Subsequent studies indicated that autophagy activation in the liver causes tissue destruction and regeneration cycles, resulting in the emergence of progenitor cells from hepatocytes, thereby driving the early stages of liver tumorigenesis (35). Consistent with these studies, western blot and immunofluorescence analysis in present study revealed that HBx induced cell autophagy in liver cancer cells (Figs. 3 and S4). These results signified that autophagy activation might be essential to the occurrence of HBV-associated liver cancer. The present findings also demonstrated that HBx enhanced the expression of PRC1 protein. PRC1 is a substrate of cyclin-dependent kinases and an exhibitor of E3 ubiquitin ligase activity, which participates in cell cycle regulation (36). It was found that deubiquitinating enzymes could reverse the process of protein ubiquitin degradation, affecting the occurrence and prognosis of liver cancer through tumor signaling pathways, apoptosis, autophagy and cell cycle regulation (37). However, the effect of PRC1 on autophagy in HBV-associated liver cancer formation remained unclear. It was concluded that the PRC1 gene participates in HBV-associated liver cancer development by regulating autophagy. The present study found that PRC1 gene overexpression significantly upregulated the expression of the autophagy-related protein ATG5 and increased the autophagic flux in the cytoplasm of Huh7 and HepG2 cells. *In vitro* functional and *in vivo* animal model studies revealed that silencing of the PRC1 gene or using the autophagosome inhibitor 3-MA reversed HBx-induced autophagy, resulting in rarely observed autophagic flux and autophagosomes, and promotion of cell apoptosis. The present findings indicate that the PRC1 gene plays an oncogenic role in HBx-associated HCC, and HBX affects autophagy in HCC through PRC1 (Figs. 3 and S5). The PRC1 gene could be a prognostic marker for HBV-associated HCC.

It was reported that PRC1 expression in lung cancer tissues was higher than in normal tissues (38). Furthermore, silencing the PRC1 gene in lung cancer cells suppressed their proliferating, migratory and invasive capabilities. Silencing the PRC1 gene in liver cancer significantly induced apoptosis of Hep3B and Huh7 cells (39). The current data revealed that PRC1 was overexpressed in HBV-positive liver cancer tissues and HBx-treated cell lines but was downregulated in HBV-negative liver cancer tissues because HBx was absent. High expression levels of PRC1 were associated with pathological stage III~IV, low differentiation, lymph node metastasis and AFP >400 μg/l. *In vivo* animal model experiments indicated that the HBx treatment significantly decreased IL-10, IL-4 and IL-2 production and increased IL-6, TNF-α and IFN-γ generation; silencing the PRC1 gene reversed this effect in an autophagy-dependent manner. These findings indicate that the PRC1 gene plays an oncogenic role in HBx-associated liver cancer. It might be possible to treat HBx-associated liver cancer by inhibiting the expression of the PRC1 gene. The PRC1 gene could be a prognostic marker for HBV-associated liver cancer.

In conclusion, a previously unknown relationship between autophagy and the PRC1 gene was demonstrated in HBV-associated liver cancer. HBx induced the expression of the PRC1 gene, a crucial carcinogenic factor that facilitates cell proliferation, migration and invasion in an autophagy-dependent manner. Therefore, PRC1 could serve as an important prognostic biomarker for patients with liver cancer. Manipulation of PRC1-regulated autophagy could be a potential clinical therapeutic approach for HBV-associated liver cancer.

Acknowledgements

Not applicable.

Funding

The present study was supported by the basic scientific research projects of provincial higher education institutions in Heilongjiang (grant no. 2020-KYYWFMY-0011).

Availability of data and materials

The data generated in the present study are included in the figures and/or tables of this article.

Authors' contributions

JJH, XZC, CW and FYG made substantial contributions to the conception. FYG made substantial contributions to the study design. JJH and XZC participated in the laboratory work and data analyses. JJH and FYG confirm the authenticity of all the raw data. All authors participated in drafting or revising

the content for important intellectual content, and read and approved the final version of the manuscript.

Ethics approval and consent to participate

Human studies were approved (approval no. 202052) by the Medical Ethics Committee of Hongqi Hospital Affiliated to Mudanjiang Medical University (Mudanjiang, China), and written informed consent was obtained from each participant. Animal experiments were approved (approval no. 2022-500-177) by the animal care committee at Mudanjiang Medical University (Mudanjiang, China).

Patient consent for publication

Not applicable.

Competing interests

The authors declare that they have no competing interests.

References

1. Brown ZJ, Tsilimigras DI, Ruff SM, Mohseni A, Kamel IR, Cloyd JM and Pawlik TM: Management of hepatocellular carcinoma: A review. JAMA Surg 158: 410-420, 2023.
2. Sung H, Ferlay J, Siegel RL, Laversanne M, Soerjomataram I, Jemal A and Bray F: Global cancer statistics 2020: GLOBOCAN estimates of incidence and mortality worldwide for 36 cancers in 185 countries. CA Cancer J Clin 71: 209-249, 2021.
3. Peng Z, Fan W, Zhu B, Wang G, Sun J, Xiao C, Huang F, Tang R Cheng Y, Huang Z, *et al*: Lenvatinib combined with transarterial chemoembolization as First-line treatment for advanced hepatocellular carcinoma: A phase III, randomized clinical trial (LAUNCH). J Clin Oncol 41: 117-127, 2023.
4. Yang C, Zhang H, Zhang L, Zhu AX, Bernards R, Qin W and Wang C: Evolving therapeutic landscape of advanced hepatocellular carcinoma. Nat Rev Gastroenterol Hepatol 20: 203-222, 2023.
5. Siegel RL, Miller KD, Fuchs HE and Jemal A: Cancer statistics, 2022. CA Cancer J Clin 72: 7-33, 2022.
6. Ajoolabady A, Tang D, Kroemer G and Ren J: Ferroptosis in hepatocellular carcinoma: Mechanisms and targeted therapy. Br J Cancer 128: 190-205, 2023.
7. Zhan X, Wu R, Kong XH, You Y, He K, Sun XY, Huang Y, Chen WX and Duan L: Elevated neutrophil extracellular traps by HBV-mediated S100A9-TLR4/RAGE-ROS cascade facilitate the growth and metastasis of hepatocellular carcinoma. Cancer Commun (Lond) 43: 225-245, 2023.
8. Shen C, Jiang X, Li M and Luo Y: Hepatitis virus and hepatocellular carcinoma: Recent advances. Cancers (Basel) 15: 533, 2023.
9. Costante F, Stella L, Santopaolo F, Gasbarrini A, Pompili M, Asselah T and Ponziani FR: molecular and clinical features of hepatocellular carcinoma in patients with HBV-HDV Infection. J Hepatocell Carcinoma 10: 713-724, 2023.
10. Zhou Q, Li L, Sha F, Lei Y, Tian X, Chen L, Chen Y, Liu H and Guo Y: PTTG1 reprograms asparagine metabolism to promote hepatocellular carcinoma progression. Cancer Res 83: 2372-2386, 2023.
11. Wang Z, Li N, Cai P, Zhang C, Cao G and Yin J: Mechanism of HBx carcinogenesis interaction with non-coding RNA in hepatocellular carcinoma. Front Oncol 13: 1249198, 2023.
12. Li Y, Gan L, Lu M, Zhang X, Tong X, Qi D, Zhao Y and Ye X: HBx downregulated decorin and decorin-derived peptides inhibit the proliferation and tumorigenicity of hepatocellular carcinoma cells. FASEB J 37: e22871, 2023.
13. Wu X, Ni Z, Song T, Lv W, Chen Y, Huang D, Xie Y, Huang W and Niu Y: C-Terminal truncated HBx facilitates oncogenesis by modulating cell cycle and glucose metabolism in FXR-deficient hepatocellular carcinoma. Int J Mol Sci 24: 5174, 2023.
14. You H, Zhang N, Yu T, Ma L, Li Q, Wang X, Yuan D, Kong D, Liu X, Hu W, *et al*: Hepatitis B virus X protein promotes MAN1B1 expression by enhancing stability of GRP78 via TRIM25 to facilitate hepatocarcinogenesis. Br J Cancer 128: 992-1004, 2023.
15. Dobrinić P, Szczurek AT and Klose RJ: PRC1 drives Polycomb-mediated gene repression by controlling transcription initiation and burst frequency. Nat Struct Mol Biol 28: 811-824, 2021.
16. Zhu P, Cui N, Song ZY, Yong WX, Luo XX, Wang GC, Wang X, Wu YN, Xu Q, Zhang LM, *et al*: PRC1 plays an important role in lung adenocarcinoma and is potentially targeted by fostamatinib. Eur Rev Med Pharmacol Sci 26: 8924-8934, 2022.
17. Bu H, Li Y, Jin C, Yu H, Wang X, Chen J, Wang Y, Ma Y, Zhang Y and Kong B: Overexpression of PRC1 indicates a poor prognosis in ovarian cancer. Int J Oncol 56: 685-696, 2020.
18. Huang R, Liu J, Li H, Zheng L, Jin H, Zhang Y, Ma W, Su J, Wang M and Yang K: Identification of hub genes and their correlation with immune infiltration cells in hepatocellular carcinoma based on GEO and TCGA databases. Front Genet 12: 647353, 2021.
19. Luo HW, Chen QB, Wan YP, Chen GX, Zhuo YJ, Cai ZD, Luo Z, Han ZD, Liang YX and Zhong WD: Protein regulator of cytokinesis 1 overexpression predicts biochemical recurrence in men with prostate cancer. Biomed Pharmacother 78: 116-120, 2016.
20. Livak KJ and Schmittgen TD: Analysis of relative gene expression data using real-time quantitative PCR and the 2(-Delta Delta C(T)) method. Methods 25: 402-408, 2001.
21. Li M, Xiao Y, Liu P, Wei L, Zhang T, Xiang Z, Liu X, Zhang K, Zhong Q and Chen F: 4-Methoxydalbergione inhibits esophageal carcinoma cell proliferation and migration by inactivating NF-κB. Oncol Rep 49: 42, 2023.
22. Liu Y, Liu X, Luo M, Li Y and Li H: HBx modulates drug resistance of Sorafenib-resistant hepatocellular carcinoma cells. Discov Med 35: 1035-1042, 2023.
23. Yu J, Li W, Hou GJ, Sun DP, Yang Y, Yuan SX, Dai ZH, Yin HZ, Sun SH, Huang G, *et al*: Circular RNA cFAM210A, degradable by HBx, inhibits HCC tumorigenesis by suppressing YBX1 transactivation. Exp Mol Med 55: 2390-2401, 2023.
24. He L, Shen H, Deng H, Zhang X, Xu Y, Shi C and Ouyang Z: Identification of critical residues in the regulatory protein HBx for Smc5/6 interaction and hepatitis B virus production. Antiviral Res 211: 105519, 2023.
25. Lei Y, Xu X, Liu H, Chen L, Zhou H, Jiang J, Yang Y and Wu B: HBx induces hepatocellular carcinogenesis through ARRB1-mediated autophagy to drive the G1/S cycle. Autophagy 17: 4423-4441, 2021.
26. Peantum J, Kunanopparat A, Hirankarn N, Tangkijvanich P and Kimkong I: Autophagy Related-protein 16-1 Up-regulated in hepatitis B Virus-related hepatocellular carcinoma and impaired apoptosis. Gastroenterology Res 11: 404-410, 2018.
27. Lin X, Li AM, Li YH, Luo RC, Zou YJ, Liu YY, Liu C, Xie YY, Zuo S, Liu Z, *et al*: Silencing MYH9 blocks HBx-induced GSK3β ubiquitination and degradation to inhibit tumor stemness in hepatocellular carcinoma. Signal Transduct Target Ther 5: 13, 2020.
28. Kimkong I and Kunanopparat A: Autophagy related protein 9A increase in hepatitis B virus-associated hepatocellular carcinoma and the role in apoptosis. World J Hepatol 12: 1367-1371, 2020.
29. Debnath J, Gammoh N and Ryan KM: Autophagy and autophagy-related pathways in cancer. Nat Rev Mol Cell Bio 24: 560-575l, 2023.
30. Gong K, Chen C, Zhan Y, Chen Y, Huang Z and Li W: Autophagy-related gene 7 (ATG7) and reactive oxygen species/extracellular signal-regulated kinase regulate tetrandrine-induced autophagy in human hepatocellular carcinoma. J Biol Chem 287: 35576-35588, 2012.
31. Sun H, Yu J, Wen Z, Wang M and Chen W: Decreased expression of Beclin-1 in patients with hepatocellular carcinoma. J BUON 24: 634-641, 2019.
32. Qian ZM, Chen YJ and Bao YX: Pharmacological mechanisms of norcantharidin against hepatocellular carcinoma. Am J Cancer Res 13: 5024-5038, 2023.
33. Vargas JNS, Hamasaki M, Kawabata T, Youle RJ and Yoshimori T: The mechanisms and roles of selective autophagy in mammals. Nat Rev Mol Cell Biol 24: 167-185, 2023.

34. Yu JL and Gao X: MicroRNA 1301 inhibits cisplatin resistance in human ovarian cancer cells by regulating EMT and autophagy. Eur Rev Med Pharmacol Sci 24: 1688-1696, 2020.
35. Kudo Y, Sugimoto M, Arias E, Kasashima H, Cordes T, Linares JF, Duran A, Nakanishi Y, Nakanishi N, L'Hermitte A, *et al*: PKCλ/ι loss induces autophagy, oxidative phosphorylation, and NRF2 to promote liver cancer progression. Cancer Cell 38: 247-262, 2020.
36. Perchey RT, Serres MP, Nowosad A, Creff J, Callot C, Gay A, Manenti S, Margolis RL, Hatzoglou A and Besson A: p27Kip1 regulates the microtubule bundling activity of PRC1. Biochim Biophys Acta Mol Cell Res 1865: 1630-1639, 2018.
37. Huang J, Zhan Y, Jiang L, Gao Y, Zhao B, Zhang Y, Zhang W, Zheng J and Yu J: Identification of the potential prognosis biomarkers in hepatocellular carcinoma: An analysis based on WGCNA and PPI. Int J Gen Med 14: 9555-9565, 2021.
38. Shi J, Hao S, Liu X, Li Y and Zheng X: Feiyiliu Mixture sensitizes EGFRDel19/T790M/C797S mutant non-small cell lung cancer to osimertinib by attenuating the PRC1/Wnt/EGFR pathway. Front Pharmacol 14: 1093017, 2023.
39. Chen W, Chen M, Zhao Z, Weng Q, Song J, Fang S, Wu X, Wang H, Zhang D, Yang W, *et al*: ZFP36 binds with PRC1 to inhibit tumor growth and increase 5-Fu chemosensitivity of hepatocellular carcinoma. Front Mol Biosci 7: 126, 2020.